J Mater Sci: Mater Electron (2008) 19:533–537
DOI 10.1007/s10854-007-9376-4

Synthesis and characterization of copper substituted lithium manganate spinels

K. R. Murali · T. Saravanan · M. Jayachandran

Received: 23 May 2007 / Accepted: 6 August 2007 / Published online: 8 September 2007

Abstract $LiCu_xMn_{2-x}O_4$ samples were synthesized by the acrylamide sol–gel process. The samples were characterized by X-ray diffraction studies, TG/DTA. Cells were made with the samples using $LiPF_6$ in propylene carbonate. Charge-Discharge and Capacity fading studies were made on the cells.

1 Introduction

$LiMn_2O_4$ spinel materials are a very attractive choice as cathode materials for lithium–ion rechargeable batteries due to their economical and environmental advantages over the current state of the art $LiCoO_2$. Previous reports by Tarascon et al. [1] and Thackarey and co-workers [2] demonstrated that addition of excess Li to the spinel ($Li_{1+x}Mn_{2-x}O_4$) improves the cathode cycle life, along with a concomitant decrease in the observed capacity. The capacity loss was reported to be $148(1 - 3x)$ mAh/gm [2]. New method for synthesis and surface modification of $LIMn_2O_4$ spinel and capacity fading studies have been recently reported [3–5]. Detailed analysis of this effect in the context of Li–Mn–O phase diagram related to $LiMn_2O_4$–$Li_4Mn_5O_{12}$–$Li_2Mn_4O_9$ cathode materials has been also reported by Xia et al. [6]. Another approach involves the substitution of a second transition element instead of Mn in the spinel oxide matrix, obtaining a general composition of $LiM_xMn_{2-x}O_4$. Attempts to substitute Mn with elements such as Co, Mg, Cr, Ni, Fe, Ti and Zn have been reported previously [7–9]. Initial results on these materials reported a lower capacity in the 4.1 V potential plateau compared with $LiMn_2O_4$ spinel [7–9]. However, a significant improvement in cycle life was reported with Ni, Co^{6+}, and Cu substituted sample materials [10–12]. Later studies showed that some of these mixed oxide spinels possess a higher voltage plateau between 4.5 V and 5.0 V, as was reported with Cu [10, 11], Ni [12–14], Cr [15], Fe [16, 17]. Earlier Cu substituted spinel was synthesized by the solid-state reaction method and sol gel method. In the solid-state reaction method [11], lithium hydroxide was mixed with required amounts of CuO and MnO_2 for a given stoichiometry and then heated for 18 h in air at 750 °C. In the sol gel method [11], acetates of copper, manganese and lithium were dissolved in deionized water and to this ammonium hydroxide was added. The mixture was stirred with gentle heating for 2 h and then concentrated to dryness on a rotary evaporator. The resulting powder was then divided into four parts and heated for 18 h in air at 350, 500, 600 and 750 °C, respectively.

In this study, Copper doped lithium manganate was synthesized by a sol gel method using acrylamide. The acrylamide sol–gel route was employed in this investigation to synthesize nanocrtstalline powder, since our earlier experience with the synthesis of lanthanates and mixed oxide semiconductors using the acrylamide route resulted in the formation of nanocrystalline powder.

2 Experimental

$LiCu_xMn_{2-x}O_4$ $(0 < x < 0.5)$ powders were prepared according to the procedure shown in Fig. 1. Stoichiometric amounts of lithium acetate, cupric nitrate and manganese

K. R. Murali (✉) · T. Saravanan · M. Jayachandran
Electrochemical Materials Science Division, Central Electrochemical Research Institute, Karaikudi 630 006, India
e-mail: muraliramkrish@gmail.com

nitrate (AR grade) salts were completely dissolved in de-ionized water. An aqueous solution of citric acid was mixed with the above mixture as chelating agent. The mixture was stirred continuously and the pH was adjusted to 6.5 by the slow addition of NH_4OH. The temperature of the solution was maintained at 70 °C. Gelling agents in the form of monoacrylamide and N–N′ methylene bis acrylamide, followed by ammonium persulphate were added to the solution. A transparent blue gel was obtained. The gel was then initially heated at 300 °C for 6 h to remove the organic material. The resulting powder was calcined at 600 °C for 8 h to get a porous black powder. Fine powders were obtained by thorough grinding in an agate mortar. For the fabrication of cells, the powders were mixed with 10% carbon black and 5% (polytetra fluoro ethylene—PTFE) and pressed onto a nickel mesh of area 1 cm^2 applying a pressure of 5 tons. The electrodes were dried in vacuum at 120 °C for 6 h before use. The electrolyte used was $LiPF_6$ in propylene carbonate. Atomic absorption spectrometry was studied using Perkin Elmer instrument. X-ray diffraction studies were made using JEOL X-ray diffractometer with CuK_α radiation. TG/DTA studies were made on a PL Thermal Science STA 1500 instrument.

3 Results and discussion

Atomic absorption spectrometry was employed for estimation of compositional parameters of copper doped $LiMn_2O_4$ spinel oxides which is shown in the Table 1. Figure 2 shows the TGA/DTA pattern for copper substituted $LiMn_2O_4$ spinel oxide for $x = 0.5$ in $LiCu_xMn_{2-x}O_4$. From DTA, it is observed that at around 115.11 °C a small endotherm which corresponds to the release of adsorbed lattice water with mass loss of less than 1% as shown in TGA. DTA shows an exotherm at 522.76 °C with the mass loss of 70% indicating the formation of single-phase compound.

Figure 3 shows the X-ray diffraction pattern for the samples prepared by the sol–gel technique. The observed peaks could be indexed as a pure cubic spinel phase. The X-ray diffraction pattern for samples from $x = 0.1$ to 0.5 show the well-defined peaks which corresponds to (111), (311), (222), (400), (551), (440). The peaks were well-defined and show crystallinity of the samples. Samples were heat-treated at different steps. Initial heating to 300 °C shows the spinel (400) peak and the impure Mn_2O_3 phase. On subsequent firing to 600 °C for 8 h reduced the Mn_2O_3 phase content and resulted in single phase copper substituted lithium manganate. The lattice parameter "a" of $LiMn_{2-x}CuxO_4$ ($x = 0.1$–0.5) spinel structures show the variation with composition "x". On increasing the substitution, the value of "a" decreases from 8.23 Å ($x = 0.1$ in $LiMn_{2-x}Cu_xO_4$ through 8.212 Å in $x = 0.3$–8.199 Å for $x = 0.5$. This indicates that the effective substitution of Cu^{2+} ions in the spinel network in place of Mn^{3+} ions which facilitates the charge neutrality of the samples. The above trend is as shown in Table 2. Charge/discharge cycling of Li/$LiMn_{2-x}Cu_xO_4$ cells was limited up to 5.1 V,

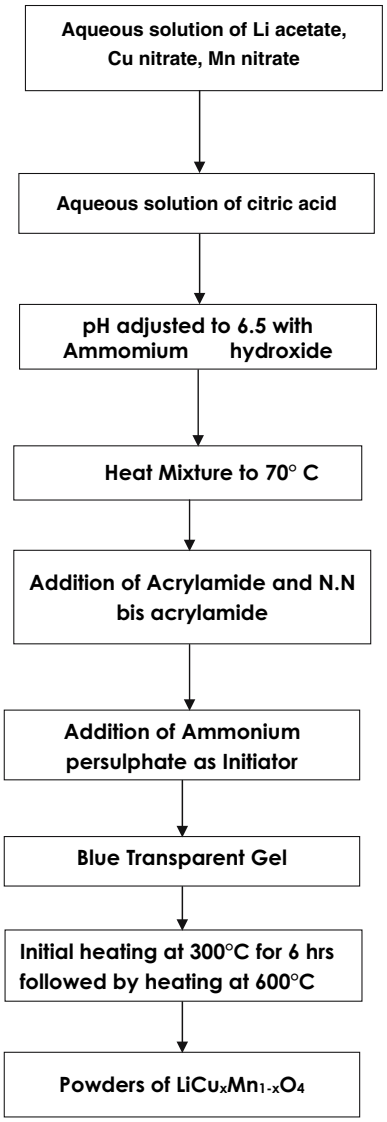

Fig. 1 Flow chart for synthesizing $LiCu_xMn_{2-x}O_4$ powders

Table 1 Composition of copper doped $LiMn_2O_4$ oxides

Theoretical formula	Li/Mn	Cu/Mn	Experimentally obtained
$LiCu_{0.1}Mn_{1.9}O_4$	0.518	0.057	$Li_{0.99}Cu_{0.11}Mn_{1.89}O_4$
$LiCu_{0.2}Mn_{1.8}O_4$	0.541	0.110	$Li_{0.99}Cu_{0.2}Mn_{1.8}O_4$
$LiCu_{0.3}Mn_{1.7}O_4$	0.585	0.183	$Li_{0.99}Cu_{0.31}Mn_{1.69}O_4$
$LiCu_{0.4}Mn_{1.6}O_4$	0.616	0.251	$Li_{0.88}Cu_{0.4}Mn_{1.6}O_4$
$LiCu_{0.5}Mn_{1.5}O_4$	0.660	0.326	$Li_{0.99}Cu_{0.49}Mn_{1.51}O_4$

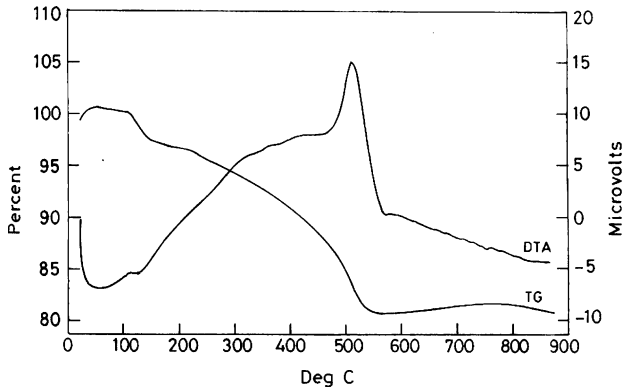

Fig. 2 TGA/DTA data of $LiCu_{0.5}Mn_{1.5}O_4$ powder

because of the possibility of electrolyte oxidation above this potential. The discharge capacity of $LiMn_{2-x}Cu_xO_4$ electrodes with Li/Li^+ anodes showing the reduction

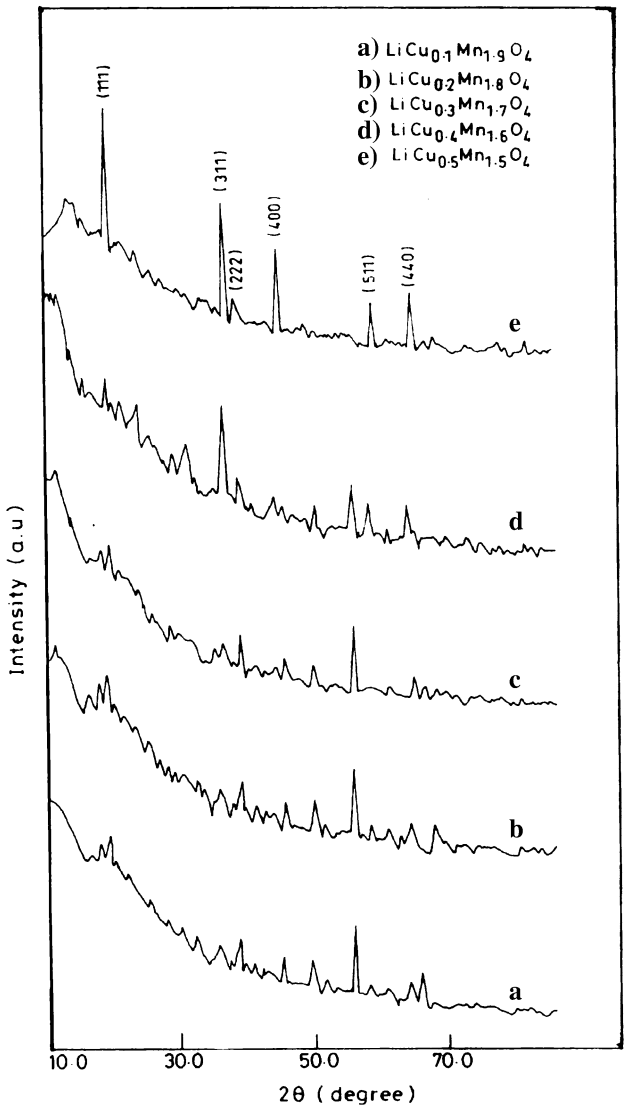

Fig. 3 XRD pattern of $LiCu_xMn_{2-x}O_4$ powders

Table 2 Unit cell parameters of $LiCu_xMn_{2-x}O4$

Composition (x)	"a" (Å)
0.1	8.230
0.2	8.221
0.3	8.212
0.4	8.205
0.5	8.199

behaviour from 120 mAh/g for $x = 0.1$–70 mAh/g for $x = 0.5$ (Fig. 4). Discharge capacity of cells with increasing composition of x in Cu-doped spinel is attributed to the fact that increased Cu^{2+} resulted to Mn^{4+} ions, which could deliver only less capacity. Mn^{3+} ion concentration is more in less doped spinel compounds and the capacity retention is more. The cycling performance of $LiCu_xMn_{2-x}O_4$ cathodes with Li anodes is as shown in Fig. 5. The obtained discharge capacity is cycled between 5.1 V and 3.3 V. During the cycling process as shown in Fig. 6, the sample with $x = 0.5$ shows higher cycle life and more capacity retention than that of other compositions. It is clear that copper substitution has two major effects on the electrochemistry of the spinel electrode that can be interpreted in terms of the coordination and oxidation state of the copper ions. If copper substitution is mimicked to Amine's nickel-substituted analog, $Li[Mn_{1.5}Ni_{0.5}]O_4$ [14] the copper ions would all be divalent and the available capacity decreases as the amount of copper in the spinel increases. However, electrodes with higher copper content showed significantly improved capacity retention during cycling. For example, "$Li/LiMnCu_{0.1}Mn_{1.9}O_4$" cells show an average, an initial capacity of 105 mAh/g, which decreases to 95 mAh/g after 60 cycles, reflecting whereas "$Li/LiCu_{0.5}Mn_{1.5}O_4$" cells show an initial capacity of 60 mAh/g that fades to 52 mAh/g over the same number of cycles. Some capacity loss may be attributed to electrolyte oxidation, particularly at potentials above 5 V. The intensity ratio I_{311}/I_{400} is

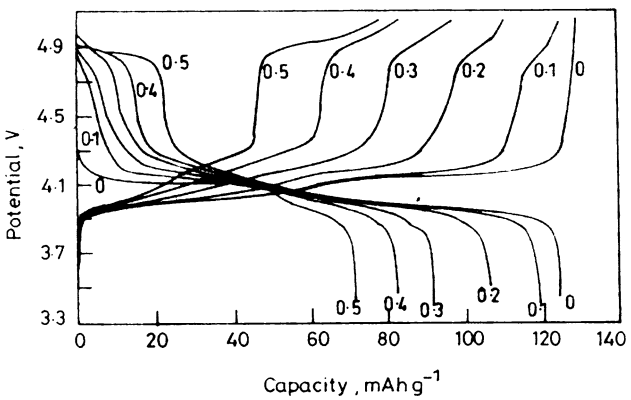

Fig. 4 Charge–discharge behaviour of $LiCu_xMn_{2-x}O_4$ cells ($x = 0.1$–0.5)

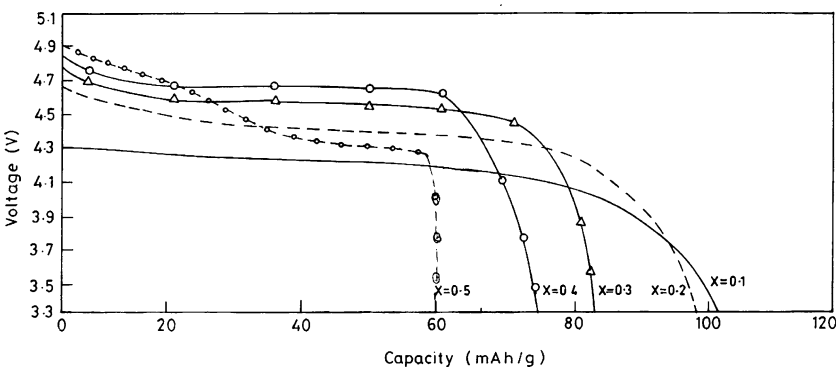

Fig. 5 Capacity fading of $LiCu_xMn_{2-x}O_4$ cells (x = 0.1–0.5)

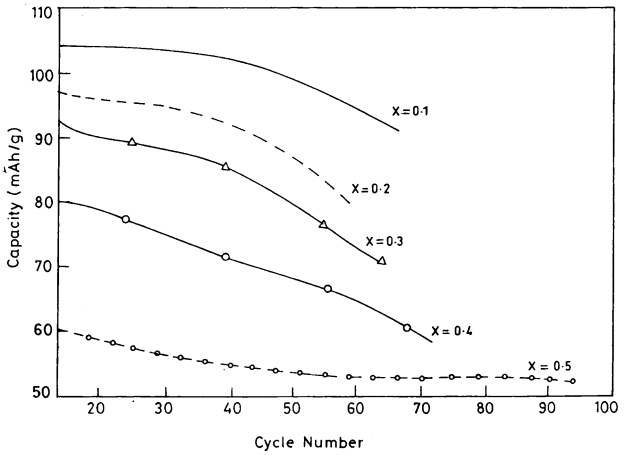

Fig. 6 Potential–capacity curves of $LiCu_xMn_{2-x}O_4$ cells (x = 0.1–0.5)

considered to be sensitive to the cation distribution, which depends upon the concentration of doping. Thus, the diffraction data proved that the synthesized samples have been formed with cubic spinel structure. The electrochemical data shown in Fig. 4 is clearly inconsistent with a spinel electrode with the simple cation arrangement in $Li[Mn_{1.5}Cu_{0.5}]O_4$. The data imply a different cation arrangement and charge distribution in the structure of the spinel electrode. The relatively large capacity that is obtained between 3.9 V and 4.4 V for $LiMn_{2-x}Cu_xO_4$ compounds with small x is associated with a large Mn^{3+} concentration on the octahedral sites. The relatively low capacity that is obtained at 4.9 V but which increases with increasing x, and the fact that the overall achievable capacity declines sharply with increasing x is consistent with increasing Cu^{2+} and Mn^{4+} concentrations in the spinel samples. Figure 5 shows the cycling performance in terms of discharge/charge capacity obtained between 4.9 V and 3.3 V, expressed in mAh/g versus cycle number for the series of $LiMn_{2-x}Cu_xO_4$ electrodes ($0.1 < x < 0.5$). In a spinel structure with the cation distribution $Li[Mn_{1.5}Cu_{0.5}]O_4$, charge neutrality is obtained when the manganese ions are all tetravalent and the copper ions are all divalent. Replacement of copper by lithium on the octahedral sites results in $Li_4Mn_5O_{12}$ (or in spinel notation $Li[Mn_{1.67}O_{0.33}]0_4$) in which charge neutrality is achieved by increasing the Mn^{4+} content to compensate for the monovalent lithium ions. These two compounds are, in principle, the end members of a possible solid-solution system $Li[Mn_{1.5-x}Cu_{0.5-3x}Li_{2x}]\ O_4$ ($0.1 \leq$ or ≤ 0.167). In this solid-solution system it would also be possible for lithium and copper ions to exchange on the tetrahedral sites. Structural refinements of such complex systems are difficult, particularly when three different cation types are disordered over one crystallographically independent site. The copper substituted spinels indicate high voltage output upto $x = 0.2$ due to the availability of large concentration of Mn^{3+}, as the "x" value increases further, the concentration of Cu^{2+} and Mn^{4+} ions increase resulting in difficulty for intercalation and deintercalation of Lithium during cycling. Hence, cathodes with low Cu substitution has to be used for lithium battery work. The results of this investigation agree well with the earlier results on copper substituted spinels [11].

4 Conclusion

The results of this investigation clearly indicate that high voltage cathodes can be synthesized with low copper concentrations at a low temperature and lower heating periods. The cycling behaviour is comparable with earlier reports.

References

1. J.M. Tarascon, F. Coowar, G. Amatuci, F.K. Shokoohi, D.G. Guyomard, J. Power Sources **54**, 103 (1995)
2. R.J. Gummow, A. de Kock, M.M. Thackeray, Solid State Ion **69**, 59 (1994)
3. H.-W. Chan, J.-G. Duh, S.-R. Sheen, S.-Y. Tsai, C.-R. Lee, Surface Coat. Technol. **200**, 1330 (2005)
4. J.T. Son, H.G. Kim, Y.J. Park, Electrochimica Acta **50**, 453 (2004)

5. L. Yang, M. Takahashi, B. Wang, Electrochimica Acta **51**, 3228 (2006)
6. Y. Xia, M. Yoshio, J. Electrochem. Soc. **144**, 4186 (1997)
7. J.M. Tarascon, E. Wang, F.K. Shokoohi, W.R. McKinnon, S. Colson, J. Electrochem. Soc. **138**, 2859 (1991)
8. R. Bittihn, R. Herr, D. Hoge, J. Power Sources **44**, 409 (1993)
9. L. Guahua, H. Ikuta, T. Uchida, M. Wakihara, J. Electrochem. Soc. **143**, 178 (1996)
10. Y. Ein-Eli W.F. Howard Jr., J. Electrochem. Soc. **144**, L205 (1997)
11. Y. Ein-Eli, W.F. Howard Jr., S.H. Lu, S. Mukerjee, J. McBreen, J.T. Vaughey, M.M. Thackeray, J. Electrochem. Soc. **145**, 1238 (1998)
12. Y. Ein-Eli, R.C. Urian, W. Wen, S. Mukerjee, Electrochimica Acta **50**, 1931 (2005)
13. Q. Zhong, A. Banakdarpour, M. Zhang, Y. Gao, J.R. Dahn, J. Electrochem. Soc. **144**, 205 (1997)
14. K. Amine, H. Tukamoto, H. Yasuda, Y. Fujita, J. Electrochem. Soc. **143**, 1607 (1996)
15. J. Dahn, T. Zheng, C.L. Thomas, J. Electrochem Soc. **145**, 851 (1998)
16. C. Sigala, D. Guyomard, A. Verbaere, Y. Piffard, M. Tournoux, Solid State Ion **81**, 167 (1995)
17. T. Ohzuku, S. Takeda, M. Iwanaga, J. Power Sources **81–82**, 90 (1999)